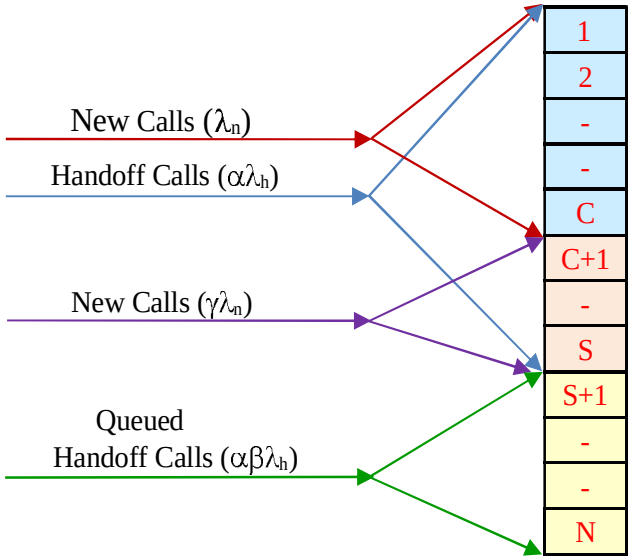

Figure 3.1: Illustration of the proposed admission control scheme.

Poisson process with mean arrival rates λ_n and λ_h, respectively.

- The call holding times (CHT) for both the streams are identical and exponentially distributed with mean $1/\mu$.

- According to the FGC scheme, when the number of busy channels is less than the fixed threshold value $C < S$, channels are equally shared among new calls and handoff calls. Once the number of occupied channels reaches the threshold C, the new calls are accepted with probability γ to achieve a trade-off between the number of new and handoff requests' service. However, if all the S channels are assigned to calls, then the incoming new calls are blocked.

- The incoming handoff calls are assigned a free channel if available. Otherwise, in case of no idle channel available in the cell, the good quality handoff calls are allowed to wait in a buffer with probability β for later transmission. The probability β here takes into account the impatience behavior of the users. However, if it chooses to join the buffer but finds not enough waiting space, then this good quality handoff call gets dropped.

- The previous studies assume that a handoff call always has an adequate signal quality however, it may not be realistic. We, therefore, consider here α to be the probability that a handoff call is of good quality signal and hence, $(1-\alpha)$ is the probability of receiving a poor quality handoff call.

3.3 Analysis of Model I

3.3.1 Markov Chain Modeling

We develop an analytical model with the help of one-dimensional CTMC. Let us denote the state of the BS as E_j which represents the sum of channels being used in the cell and the number of handoff requests in the buffer. The state transition rate diagram is shown in Fig. 3.2.

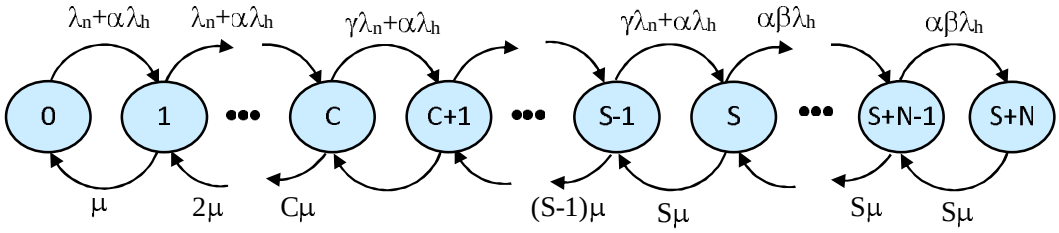

Figure 3.2: State transition diagram for model I.

In this model, we assume that any poor quality handoff call is instantly dropped; the effective arrival rate up to channel C is $(\lambda_n + \alpha\lambda_h)$ and from C to S is $(\gamma\lambda_n + \alpha\lambda_h)$. If the handoff call request finds all the S channels occupied then rather than dropping, the good signal quality handoff call is buffered with probability β until a channel is available. In view of this, the arrival rate from $S+1$ to $S+N$ is $\alpha\beta\lambda_h$.

The birth-death process is used to determine P_j which represents the steady-state probability that the BS is in state E_j. Thus using product type solution, we have

$$P_j - \begin{cases} \frac{1}{j!}\left(\frac{\lambda_n+\alpha\lambda_h}{\mu}\right)^j P_0; & 0 \le j < C \\ \frac{1}{j!}\left(\frac{\lambda_n+\alpha\lambda_h}{\mu}\right)^C \left(\frac{\gamma\lambda_n+\alpha\lambda_h}{\mu}\right)^{j-C} P_0; & C \le j < S \\ \frac{1}{S!}\left(\frac{\lambda_n+\alpha\lambda_h}{\mu}\right)^C \left(\frac{\gamma\lambda_n+\alpha\lambda_h}{\mu}\right)^{S-C} \left(\frac{\alpha\beta\lambda_h}{S\mu}\right)^{j-S} P_0; & S \le j \le S+N. \end{cases} \tag{3.1}$$

Using the normalization condition, $\sum_{j=0}^{S+N} P_j = 1$, P_0 is obtained as

$$P_0 = \left[\sum_{j=0}^{C} \frac{1}{j!} \left(\frac{\lambda_n + \alpha\lambda_h}{\mu} \right)^j + \sum_{j-C+1}^{S} \frac{1}{j!} \left(\frac{\lambda_n + \alpha\lambda_h}{\mu} \right)^C \left(\frac{\gamma\lambda_n + \alpha\lambda_h}{\mu} \right)^{j-C} + \sum_{j=S+1}^{S+N} \frac{1}{S!} \left(\frac{\lambda_n + \alpha\lambda_h}{\mu} \right)^C \left(\frac{\gamma\lambda_n + \alpha\lambda_h}{\mu} \right)^{S-C} \left(\frac{\alpha\beta\lambda_h}{S\mu} \right)^{j-S} \right]^{-1}. \tag{3.2}$$

3.3.2 Performance Measures

In this section, we give the expressions for the important performance measures as follows.

1. In this study, a new call is blocked if the arriving call finds all the channels occupied or when not admitted under the FGC policy. The *blocking probability* of a new call, B_n, is given by

$$B_n = (1-\gamma) \sum_{j-C}^{S-1} P_j + \sum_{j-S}^{S+N-1} P_j + P_{S+N}. \tag{3.3}$$

2. The (forced) *dropping probability* of a handoff call is equal to the sum of the probability of buffer being filled up and the probability that the handoff call is of poor signal quality. Thus, the probability of dropping, B_h, is given as

$$B_h = (1-\alpha) \sum_{j=0}^{S+N} P_j + \alpha\beta P_{S+N}. \tag{3.4}$$

3. The *channel utilization* is the ratio of average number of busy channels to the total number of channels available in each cell. Hence, the channel utilization, $U(S)$, is determined by

$$U(S) = \frac{1}{S} \left[\sum_{j=1}^{S-1} j P_j + S \sum_{j=S}^{j=S+N} P_j \right]. \tag{3.5}$$

4. Another effective measure of system performance is *buffer utilization*, $U(N)$. It is

expressed as

$$U(N) = \frac{N_q}{N}, \tag{3.6}$$

where N is buffer size and $N_q = \sum_{j=S+1}^{S+N} (j-S)P_j$ is mean number of calls in buffer.

3.4 Analysis of Model II

3.4.1 Markov Chain Modeling

The network service providers aim to satisfy the QoS requirements which is usually associated with minimizing handoff failure due to poor quality signal while keeping the new call blocking probability below a fixed threshold.

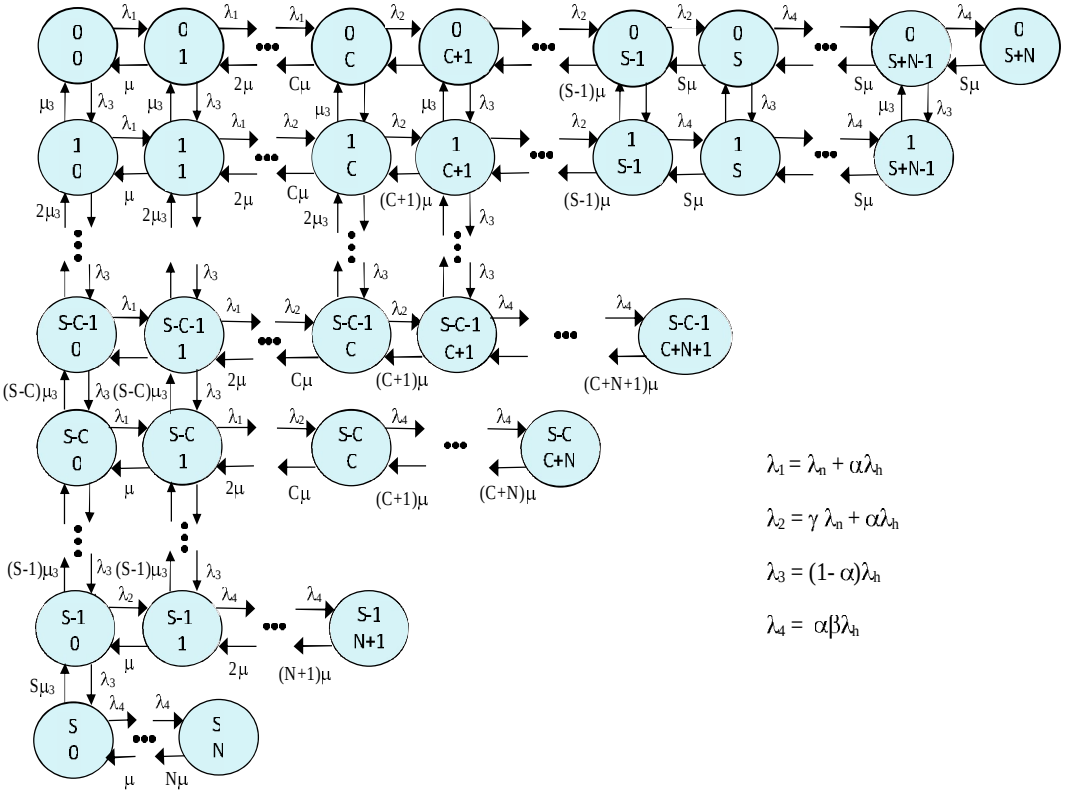

Figure 3.3: State transition diagram for model II.

The proposed model II addresses the scenario wherein a poor signal quality handoff call is not immediately dropped as in the proposed model I. Instead, such a call can be re-

handed off to some other BS system that serves better. For carrying out the performance analysis of this scheme, we analyze the two-dimensional CTMC model that incorporates poor signal quality handoff calls as well, as shown in Fig. 3.3.

The proposed model II also assumes a homogeneous multi-cellular system with the same traffic patterns. Consequently, this allows focusing on one given cell for performance analysis and the results of this reference cell are applicable to all other cells. In this model, the call completion time and the handoff time both are assumed to be random, each having exponential distribution with rate parameters μ_1 and μ_2, respectively. This, in turn, implies that the total duration of time a call spends in a cell is also random and assumed to be exponentially distributed with rate where μ, where $\mu - \mu_1 + \mu_2$. Since this model takes into account that $\bar{\alpha}$ fraction of received handoff calls are of poor signal quality, thus the receiving cell requires to quickly re-handoff these calls, when allocated a channel but cannot be sustained by the BS due to bad signal quality. The duration of time spent by a poor signal handoff call is also a random variable and assumed to have exponential distribution with rate parameter μ_3. Hence, in view of the fact that a good quality signal is likely to reside in a cell for a longer duration in comparison to poor signal quality, generally, $\mu_3 >> \mu_2$. As a consequence, the overall performance of the cellular network is enhanced by the implementation of two dimensional Markov model.

At any instant, the state of the CTMC is determined by $(i,j) \in \sigma - \{(i,j), 0 \leq i \leq S. 0 \leq j \leq S + N\}$ where i corresponds to the number of poor signal quality handoff calls being handled, and j corresponds to the number of good signal quality calls in progress. Let $P_{i,j}$ be the steady-state probability that the given cell is in state (i,j). The corresponding set of global balance equations is given by

$$(\lambda_1 + \lambda_3)P_{i,j} - \mu P_{i,j+1} + \mu_3 P_{i+1,j}; \quad (i,j) = (0,0)$$

$$(\lambda_1 + \lambda_3 + j\mu)P_{i,j} = (j+1)\mu P_{i,j+1} + \mu_3 P_{i+1,j} + \lambda_1 P_{i,j-1}; \quad i = 0, 1 \leq j \leq C-1$$

$$(\lambda_2 + \lambda_3 + j\mu)P_{i,j} = (j+1)\mu P_{i,j+1} + \mu_3 P_{i+1,j} + \lambda_1 P_{i,j-1}; \quad (i,j) = (0,C)$$

$$(\lambda_2+\lambda_3+j\mu)P_{i,j}=(j+1)\mu P_{i,j+1}+\mu_3 P_{i+1,j} + \lambda_2 P_{i,j-1};\quad i=0, C+1\le j\le S-1$$

$$(\lambda_4+\lambda_3+S\mu)P_{i,j}=(S\mu)P_{i,j+1}+\mu_3 P_{i+1,j}+\lambda_2 P_{i,j-1};\quad (i,j)=(0,S)$$

$$(\lambda_4+\lambda_3+S\mu)P_{i,j}=(S\mu)P_{i,j+1}+\mu_3 P_{i+1,j} + \lambda_4 P_{i,j-1};\ \ i=0, S+1\le j\le S+N-1$$

$$(S\mu)P_{i,j}=\lambda_4 P_{i,j-1};\quad (i,j)=(0,S+N)$$

$$(\lambda_1+i\mu_3+\lambda_3)P_{i,j}-\mu P_{i,j+1}+\lambda_3 P_{i-1,j}+(i+1)\mu_3 P_{i+1,j};\ \ 1\le i\le C-1, j=0$$

$$(\lambda_4+i\mu)P_{i,j}-\mu P_{i,j+1}+\lambda_3 P_{i-1,j};\quad (i,j)=(S,0)$$

$$(\lambda_1+i\mu_3+\lambda_3+j\mu)P_{i,j}=(j+1)\mu P_{i,j+1}+\lambda_3 P_{i-1,j}+(i+1)\mu_3 P_{i+1,j} + \lambda_1 P_{i,j-1};\quad 1\le i\le C-2, 1\le j\le C-i-1$$

$$(\lambda_2+i\mu_3+\lambda_3+j\mu)P_{i,j}=(j+1)\mu P_{i,j+1}+\lambda_3 P_{i-1,j}+(i+1)\mu_3 P_{i+1,j} + \lambda_1 P_{i,j-1};\quad 1\le i\le C-1, i+j-C$$

$$(\lambda_2+i\mu_3+\lambda_3+j\mu)P_{i,j}=(j+1)\mu P_{i,j+1}+\lambda_3 P_{i-1,j}+(i+1)\mu_3 P_{i+1,j} + \lambda_2 P_{i,j-1};\quad 1\le i\le C, C-i+1\le j\le S-i-1$$

$$(\lambda_4+i\mu_3+\lambda_3+j\mu)P_{i,j}=(j+1)\mu P_{i,j+1}+\lambda_3 P_{i-1,j}+(i+1)\mu_3 P_{i+1,j} + \lambda_2 P_{i,j-1}; 1\le i\le S-1, i+j-S$$

$$(\lambda_4+i\mu_3+\lambda_3+j\mu)P_{i,j}=(j+1)\mu P_{i,j+1}+\lambda_3 P_{i-1,j}+(i+1)\mu_3 P_{i+1,j} + \lambda_4 P_{i,j-1};\ 1\le i\le S-1, S-i+1\le j\le S-i+N-1$$

$$(i\mu_3+j\mu)P_{i,j}-\lambda_3 P_{i-1,j}+\lambda_4 P_{i,j-1};\quad 1\le i\le S, i+j-S+N$$

$$(\lambda_4+i\mu_3+j\mu)P_{i,j}=(j+1)\mu P_{i,j+1}+\lambda_3 P_{i-1,j} + \lambda_4 P_{i,j-1};\quad i=S, 1\le j\le S-i+N-1$$

where $\lambda_1-\lambda_n+\alpha\lambda_h$; $\lambda_2-\gamma\lambda_n+\alpha\lambda_h$; $\lambda_3=(1-\alpha)\lambda_h$; $\lambda_4-\alpha\beta\lambda_h$. By solving the balance equations of the Markov Chain, the steady-state transition probabilities $P_{i,j}$ are

derived as

$$P_{i,j} = \begin{cases} \frac{1}{j!}\left(\frac{\lambda_1}{\mu}\right)^j P_{0,0}; & i=0, 0<j\leq C \\ \frac{1}{j!}\left(\frac{\lambda_1}{\mu}\right)^C \left(\frac{\lambda_2}{\mu}\right)^{j-C} P_{0,0}; & i=0, C+1\leq j\leq S \\ \frac{1}{S!}\left(\frac{\lambda_1}{\mu}\right)^C \left(\frac{\lambda_2}{\mu}\right)^{S-C}\left(\frac{\lambda_4}{\mu}\right)^{j-S} P_{0,0}; & i=0, S+1<j\leq S+N \\ \frac{1}{i!}\left(\frac{\lambda_2}{\mu_3}\right)^i \frac{1}{j!}\left(\frac{\lambda_1}{\mu}\right)^j P_{0,0}; & 1\leq i\leq C-1, 1\leq j\leq C-i-1 \\ \frac{1}{i!}\left(\frac{\lambda_2}{\mu_3}\right)^i \left(\frac{{\lambda_1}^{C-i}\lambda_2{}^{j-C+i}}{j!\mu^j}\right) P_{0,0}; & 1\leq i\leq C-1, C-i\leq j\leq S-i \\ \frac{1}{i!}\left(\frac{\lambda_2}{\mu_3}\right)^i \left(\frac{{\lambda_1}^{C-i}\lambda_2{}^{S-C+i}\lambda_4{}^{j-S}}{(S-i)!\,S^{j-S+i}\mu^j}\right) P_{0,0}; & 1\leq i\leq C-1, S-i+1\leq j\leq S-i+N \\ \frac{1}{i!}\left(\frac{\lambda_2}{\mu_3}\right)^i \left(\frac{\lambda_2^j}{j!\mu^j}\right) P_{0,0}; & C\leq i\leq S-1, 1\leq j\leq S-i \\ \frac{1}{i!}\left(\frac{\lambda_2}{\mu_3}\right)^i \left(\frac{\lambda_2{}^{S-i}\lambda_4{}^{j-S+i}}{(S-i)!\,S^{j-S+i}\mu^j}\right) P_{0,0}; & C\leq i\leq S, S-i+1\leq j\leq S-i+N \\ \frac{1}{i!}\left(\frac{\lambda_2}{\mu_3}\right)^i P_{0,0}; & 1\leq j\leq S, j=0 \end{cases} \tag{3.7}$$

Using the normalization condition $\sum_{i=0}^{S}\sum_{j=0}^{S+N-i} P_{i.j} = 1$, the probability that all channels are free, $P_{0,0}$ is computed as

$$\begin{aligned} P_{0,0} - \Bigg[& 1 + \sum_{j=0}^{C}\frac{1}{j!}\left(\frac{\lambda_1}{\mu}\right)^j + \sum_{j-C+1}^{S}\frac{1}{j!}\left(\frac{\lambda_1}{\mu}\right)^C\left(\frac{\lambda_2}{\mu}\right)^{j-C} \\ & + \sum_{j=S+1}^{S+N}\frac{1}{S!}\left(\frac{\lambda_1}{\mu}\right)^C\left(\frac{\lambda_2}{\mu}\right)^{S-C}\left(\frac{\lambda_4}{\mu}\right)^{j-S} + \sum_{i=1}^{C-1}\sum_{j=1}^{C-i-1}\frac{1}{i!}\left(\frac{\lambda_3}{\mu_3}\right)^i\frac{1}{j!}\left(\frac{\lambda_1}{\mu}\right)^j \\ & + \sum_{i=1}^{C-1}\sum_{j=C-i}^{S-i}\frac{1}{i!}\left(\frac{\lambda_3}{\mu_3}\right)^i\left(\frac{{\lambda_1}^{C-i}\lambda_2{}^{j-C+i}}{j!\mu^j}\right) \\ & + \sum_{i=1}^{C-1}\sum_{j=S-i+1}^{S-i+N}\frac{1}{i!}\left(\frac{\lambda_3}{\mu_3}\right)^i\left(\frac{{\lambda_1}^{C-i}\lambda_2{}^{S-C+i}\lambda_4{}^{j-S}}{(S-i)!\,S^{j-S+i}\mu^j}\right) + \sum_{i=C}^{S-1}\sum_{j=1}^{S-i}\frac{1}{i!}\left(\frac{\lambda_3}{\mu_3}\right)^i\left(\frac{\lambda_2^j}{j!\mu^j}\right) \\ & + \sum_{i-C}^{S}\sum_{j-S-i+1}^{S-i+N}\frac{1}{i!}\left(\frac{\lambda_3}{\mu_3}\right)^i\left(\frac{\lambda_2{}^{S-i}\lambda_4{}^{j-S+i}}{(S-i)!\,S^{j-S+i}\mu^j}\right) + \sum_{i=1}^{S}\frac{1}{i!}\left(\frac{\lambda_3}{\mu_3}\right)^i\Bigg]^{-1}. \end{aligned} \tag{3.8}$$

3.4.2 Performance Measures

After the state probabilities are known, we now derive the performance measures of interest.

1. The new call *blocking probability*, B_n, is given by

$$B_n = (1-\gamma)\left[\sum_{i=0}^{C}\sum_{j=C-i}^{S-i-1} P_{i,j} + \sum_{i=C+1}^{S-1}\sum_{j=0}^{S-i-1} P_{i,j}\right] + \sum_{i=0}^{S}\sum_{j=S-i}^{S+N-i} P_{i,j}. \tag{3.9}$$

2. The (forced) *dropping probability* of a handoff call, B_h, is obtained as

$$B_h = (1-\alpha)\sum_{i=0}^{S}\sum_{j=S-i}^{S+N-i} P_{i,j} + \alpha\beta\sum_{i=0}^{S} P_{i,S+N-i}. \tag{3.10}$$

3. The *channel utilization*, $U(S)$, is expressed as

$$U(S) = \frac{1}{S}\left[\sum_{i=0}^{S}\sum_{j=0}^{S+N-i}(i+j)P_{i,j} + S\sum_{i=0}^{S}\sum_{j-S+1-i}^{S+N-i} P_{i,j}\right]. \tag{3.11}$$

4. *Buffer utilization*, $U(N)$, is given by

$$U(N) = \frac{N_q}{N} \tag{3.12}$$

where

$$N_q = \sum_{i=0}^{S}\sum_{j-S-i}^{S+N-i-1}(i+j-S)P_{i,j} + N\sum_{i=0}^{S} P_{i,S+N-i}. \tag{3.13}$$

5. In cellular networks, the average queueing delay defined as the ratio of the average number of calls in the buffer to the throughput of the queue is also an important measure. Herein, the *throughput* of the queue is given by

$$\tau - \lambda_h(1-B_h). \tag{3.14}$$

6. Using Little's formula by D.C. Little [200] (i.e., the expected waiting time a call spends in the queue in steady-state is equal to the product of the effective arrival rate and the expected number of calls in the queue), the mean wait time or *average queueing delay* is calculated as

$$D = \frac{N_q}{\tau}. \tag{3.15}$$

3.5 Optimization of New Call Acceptance Probability (γ^*)

In this section, we formulate a non-linear optimization problem to find the optimal value of new call acceptance probability when C number of channels are busy, where the number of channels allocated to a particular cell along with the buffer size is held fixed. The procedure takes into account that the new call blocking probability (B_n) is a monotonically decreasing function of the admission probability (γ) and the handoff dropping probability (B_h) is a monotonically increasing function of the admission probability (see e.g., Beigy and Meybodi [201]).

Here the objective is to find γ^* that minimizes the new call blocking probability, B_n subject to the hard constraint on handoff dropping probability, $B_h \leq P_h$ where P_h is the level of QoS to be satisfied for handoff calls.

$$\begin{aligned} &\text{Minimize} && B_n(\gamma) \\ &\text{subject to} && B_h(\gamma) \leq P_h, \\ & && 0 \leq \gamma \leq 1. \end{aligned} \tag{3.16}$$

The value of P_h is pre-specified by the quality requirement of service of the network which usually ranges from $1-5$ % and 2 % percent being the most commonly used value (see, Beigy and Meybodi [202]). In order to find γ^*, the algorithm 1 is developed. This algorithm concerned with the optimality of the solution is based on the binary search method.

Algorithm 1: Calculate optimized new call acceptance probability

Input: P_h

Output: γ^*

Initialize: $S, C, N, \lambda_n, \lambda_h, \mu, \mu_3, \alpha, \beta$

Set $\gamma_{\text{lower}} = 0$; $\gamma_{\text{upper}} = 1$

if $B_h(\gamma_{upper}) \leq P_h$ **then**
  $\gamma^* \leftarrow \gamma_{\text{upper}}$

if $B_h(\gamma_{lower}) \geq P_h$ **then**
  $\gamma^* \leftarrow \gamma_{\text{lower}}$

while $\gamma^* \notin 0, 1$ *and* $(\gamma_{upper} - \gamma_{lower}) \leq 0.0001$ **do**
  Set $\gamma^* \leftarrow (\gamma_{\text{upper}} + \gamma_{\text{lower}})/2$
  if $B_h(\gamma^*) > P_h$ **then**
    $\gamma_{\text{upper}} \leftarrow \gamma^*$
  else
    $\gamma_{\text{lower}} \leftarrow \gamma^*$

3.6 Numerical Results and Discussion

In order to examine the effect of different parameters on various performance indices such as channel utilization $U(S)$, buffer utilization $U(N)$, dropping probability B_h and blocking probability B_n, numerical results of both the models have been presented. The default parameters are taken as $S = 15, C = 8, N = 3, \lambda_h = 20, \lambda_n = 5, \mu = 2, \mu_3 = 1, \alpha = 0.6, \beta = 0.2, \gamma = 0.2$.

The effects of handoff arrival rate, λ_h on new call blocking probability, B_n and handoff call dropping probability, B_h under different values of queueing probability for good quality handoff calls, β have been illustrated for model I in Figs. 3.4(a) and 3.4(b) and for model II in Figs. 3.4(c) and 3.4(d), respectively. It is observed that an increase in λ_h as well as in parameter β leads to more blocking of new calls and more dropping of handoff calls.

Furthermore, it is noted that the proposed model II exhibits much improvement in the dropping probability of handoff calls under all values of β . This is because, in the

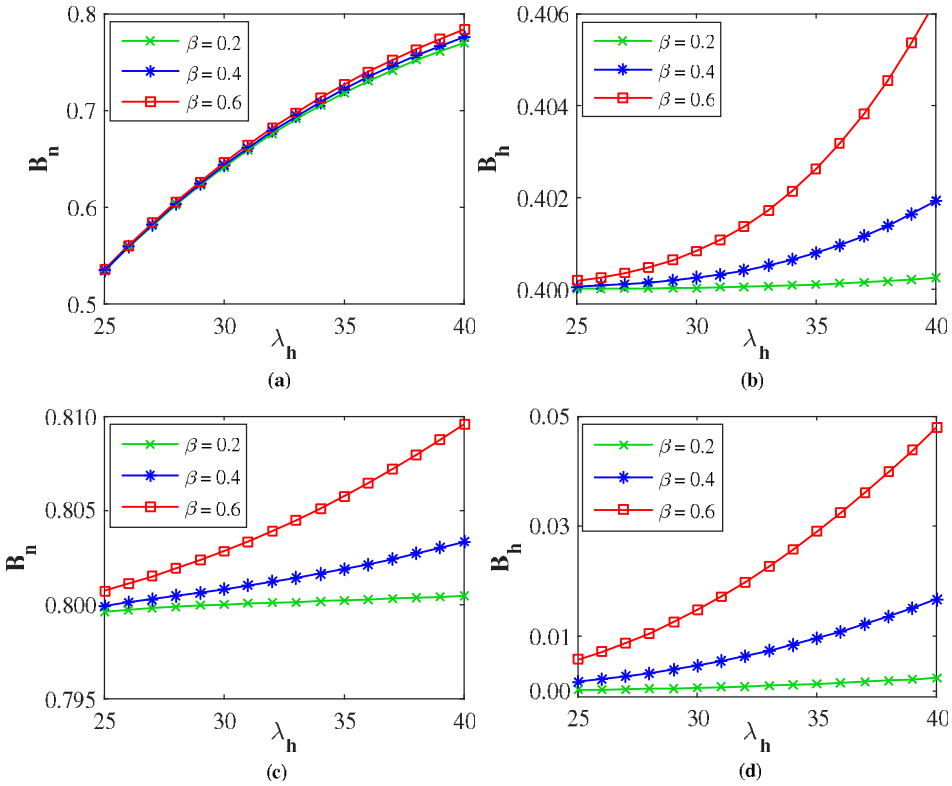

Figure 3.4: Effect of handoff arrival rate on (a) blocking probability and (b) dropping probability of model I; (c) blocking probability and (d) dropping probability of model II, for different queueing probabilities.

proposed model II instead of immediate dropping, a poor signal quality handoff call is re-hand off to neighboring cells and thereby, reduces the probability of dropping of handoff calls. Hence, choosing a proper value of probability to wait in the buffer, acts as a trade-off between more or less dropping of handoff calls.

Fig. 3.5 reveals the sensitivity of channel size, S on the blocking probability based on different values of threshold, C for model I (Fig. 3.5(a)) and model II (Fig. 3.5(b)). It is clear that as channel size S increases, the blocking probability for model II reduces quite moderately as compared to the model I because the channels being available becomes more in number. We also observe that for a constant admissible value of channel size, with the increment in threshold C, the new call blocking probability lowers down significantly irrespective of the model. That makes logic as the number of new calls being accepted

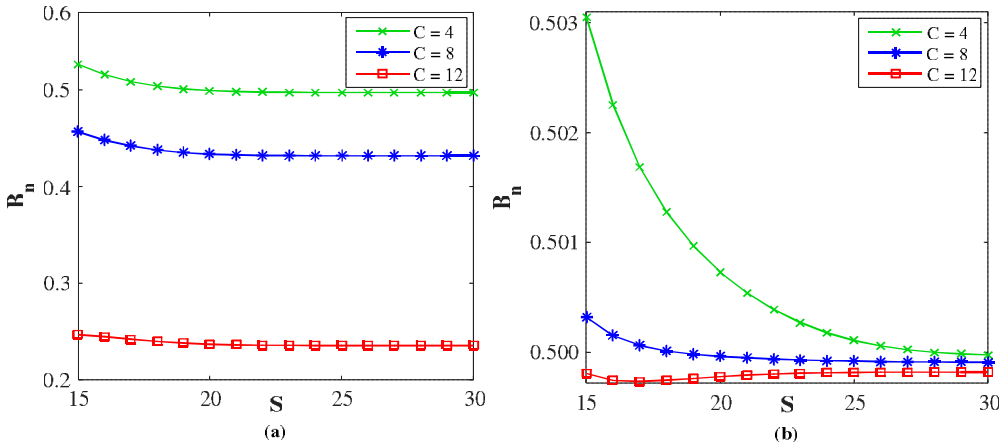

Figure 3.5: Effect of channel size on blocking probability of (a) model I; (b) model II, for different threshold values.

gets more with an increase in the value of C. Consequently, choosing a proper threshold value plays a major role in achieving better performance results.

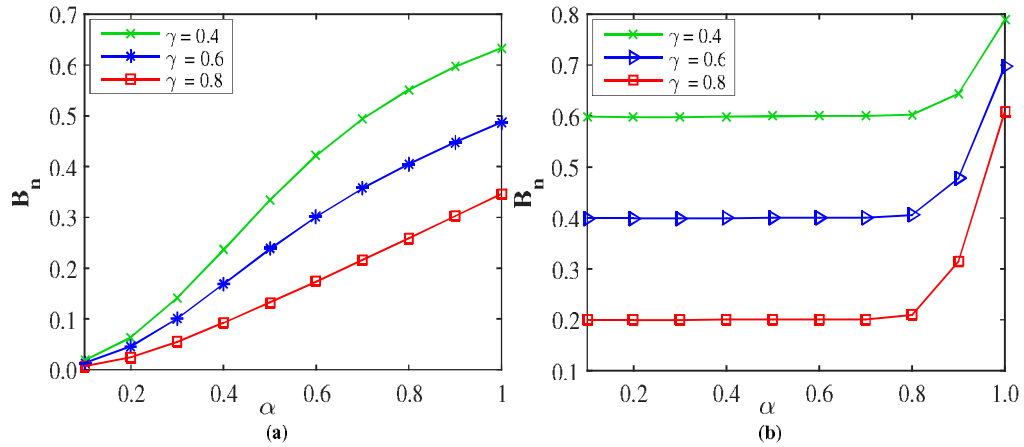

Figure 3.6: Effect of signal quality probability on blocking probability of (a) model I; (b) model II, for different acceptance probabilities.

The impact of signal quality, α on the new call blocking probabilities with different values of acceptance probability, γ for model I is shown in Fig. 3.6(a) and for model II in Fig. 3.6(b). It is noticed that for both models, the increase of signal quality α, results in higher values of the blocking probability for all values of γ. This increment is a result of more admittance of good signal quality handoff calls. However, as per our expectation,

for model II the effect of signal quality seems to be limited on blocking probability. In addition, the blocking probability decreases significantly while γ is increased, as this provides more available resources to serve new calls.

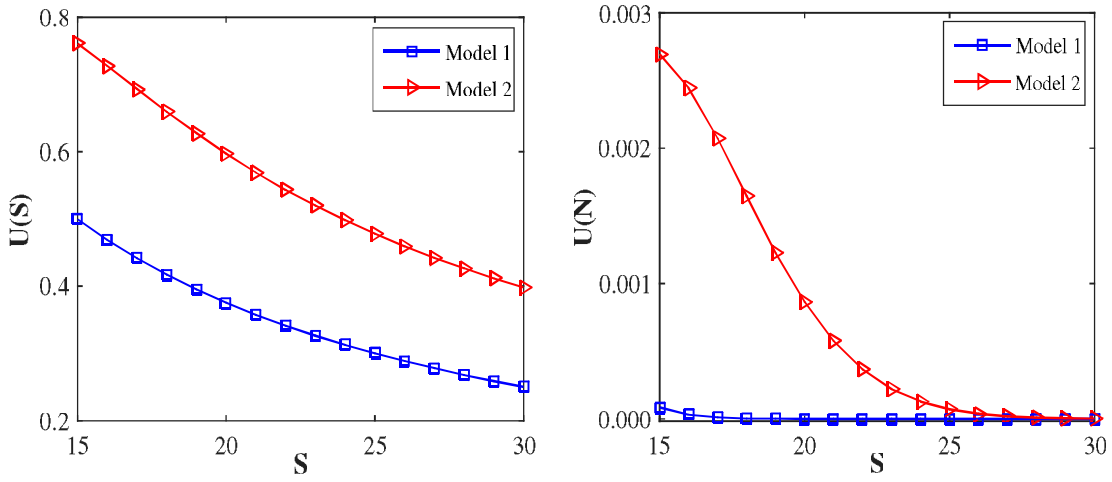

Figure 3.7: Effect of number of channels on (a) channel utilization; (b) buffer utilization.

Fig. 3.7 explains the impact of channel size, S on channel utilization (Fig. 3.7(a)) and buffer utilization (Fig. 3.7(b)) for both the models, and that matches with the realistic situation for any cellular communication network as with the increase in channel size, more number of channels gets available for allocation which leads to decrease in channel utilization. It is interesting to mark that for a constant value of channel size, the proposed model II provides better channel utilization as well as buffer utilization as compared to the proposed model I, due to utilization of more resources while re-handling of poor signal quality handoff calls. Hence, by choosing an admissible value of channel size, we can make the efficient utilization of channels.

Fig. 3.8 demonstrates the behavior of channel utilization (Fig. 3.8(a)) and buffer utilization (Fig. 3.8(b)) as a function of handoff arrival rate, λ_h under different values of handoff call buffering probability, β for both the models. It is observed that with the increasing arrival rate of handoff calls, both channel utilization and buffer utilization increase gradually for all values of β irrespective of the models. However, the channel

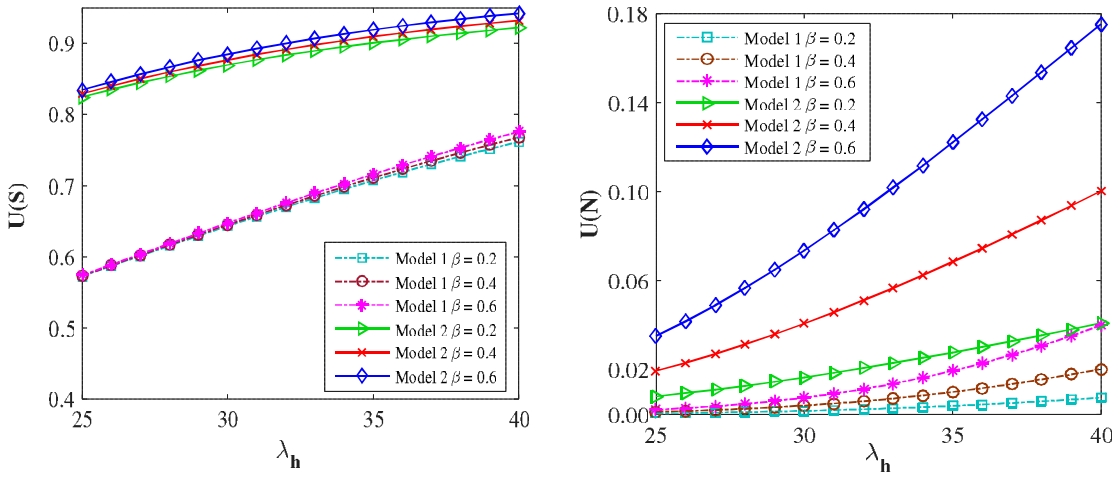

(a) (b)

Figure 3.8: Effect of handoff arrival rate on (a) channel utilization; (b) buffer utilization, for different queueing probabilities.

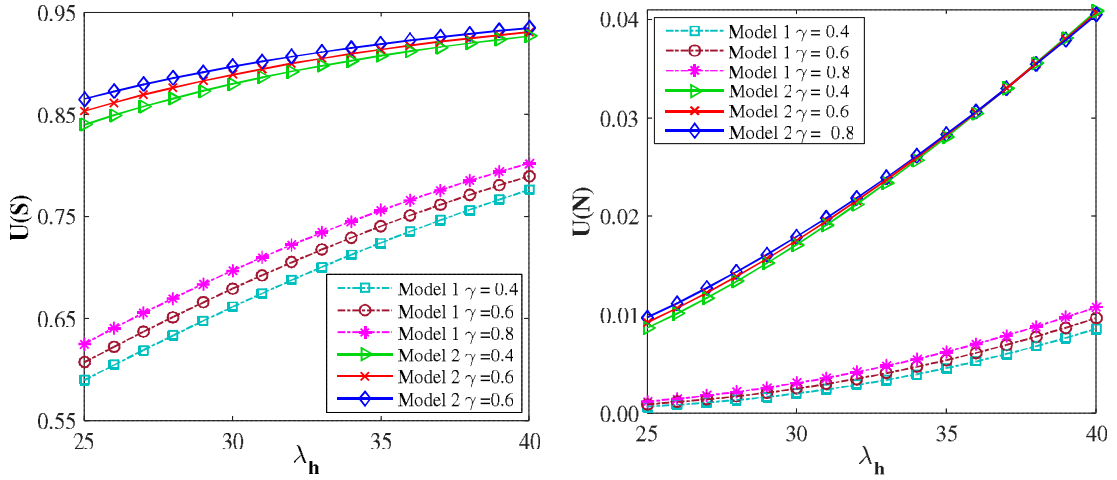

(a) (b)

Figure 3.9: Effect of handoff arrival rate on (a) channel utilization; (b) buffer utilization, for different acceptance probabilities.

utilization for model I and model II differs remarkably under various values of the parameter β whereas the buffer utilization for model II is little more in comparison to model I. It is also noticeable that buffer utilization increases with the increasing value of β but channel utilization is less affected by β. This may be explained by the fact that increase in β, increases the probability for a good quality handoff call to be queued and thereby, increases the utilization of buffer. This depicts the effectiveness of the parameter β.

The curves under different values of new call acceptance probability, γ corresponding to channel utilization (Fig. 3.9(a)) and buffer utilization (Fig. 3.9(b)) are also presented for comparison. It illustrates that both channel utilization and buffer utilization gets increase while γ is increased as more new calls are admitted. However, for model II, in heavy traffic region of handoff calls, buffer utilization seems to be invariant with respect to γ. So the dominant factor that affects utilization is the traffic load of handoff. Moreover, it is clear from the results that the proposed model II outperforms the model I.

Further, to analyze the effect of buffer employed, comparison of the proposed scheme with the scheme without any buffer is presented for model II with $\alpha = 0.75$ and $\beta = 0.6$.

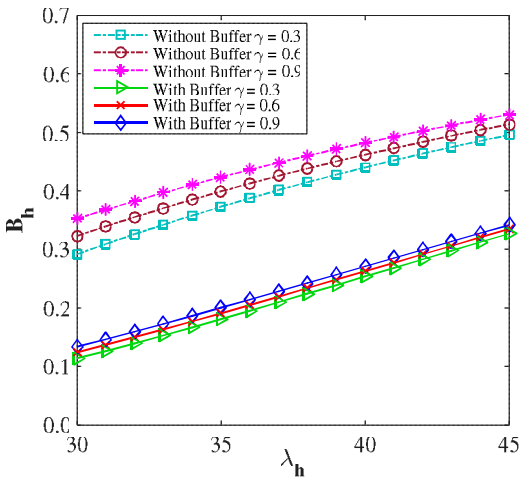

Figure 3.10: Dropping probability as a function of handoff arrival rate for different acceptance probabilities.

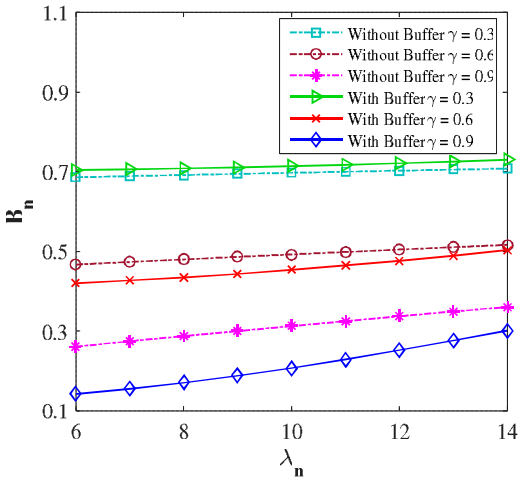

Figure 3.11: Blocking probability as a function of handoff arrival rate for different acceptance probabilities.

The variation of dropping probability and blocking probability versus arrival rates, λ_h and λ_n, respectively for different values of acceptance probability, γ is shown in Figs. 3.10 and 3.11. As is to be expected, with an increase in the new call acceptance probability, handoff call dropping probability increases whereas the new call blocking probability decreases. We notice that the proposed scheme (with buffer handoff calls) exhibits much improvement in the dropping probability of handoff calls under all values of γ, compared

with the scheme without buffer. In addition, incorporating the queueing scheme also lowers down the blocking probability of new calls and it is apparent that the decrement is more significant for higher values of γ.

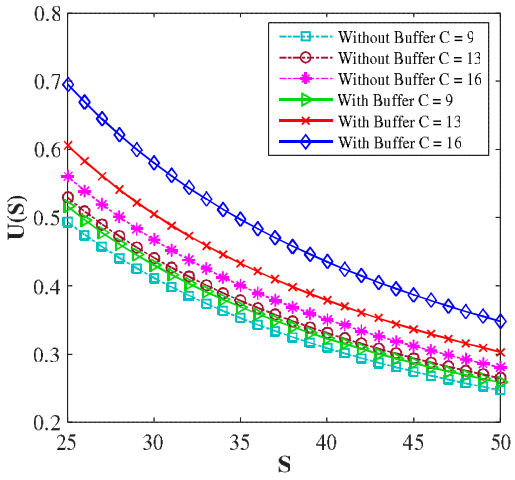

Figure 3.12: Channel utilization as a function of number of channels for different threshold values.

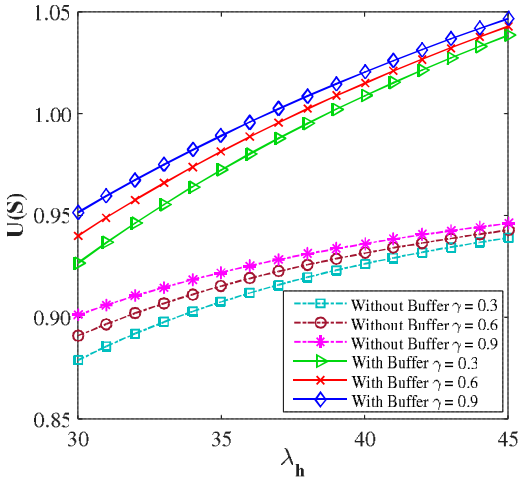

Figure 3.13: Channel utilization as a function of handoff arrival rate for different acceptance probabilities.

Fig. 3.12 illustrates the comparison of channel utilization with channel size, S for different values of threshold, C. The increase in channel size leads to the availability of more channels for allocation, which in turn, gradually decreases the channel utilization. Again, we find improvement in channel utilization utilizing the proposed scheme with buffer. It is observed that as threshold value C increases, the utilization factor increases. This is due to the fact that an increase in C allows both new and handoff calls equal access to a greater number of channels at all times. Further, the effectiveness of acceptance probability, γ on channel utilization versus handoff arrival rate, λ_h is revealed in Fig. 3.13. Higher new calls' acceptance probability will cause more calls to be served, therefore utilization factor increases with an increase in γ. Moreover, we see a remarkable difference in the channel utilization factor for the schemes with and without buffer in case of heavy traffic load.

As is to be expected, Figs. 3.14 and 3.15 depict that the buffer utilization factor increases with an increase in the handoff call arrival rate, λ_h. Also, since higher queueing

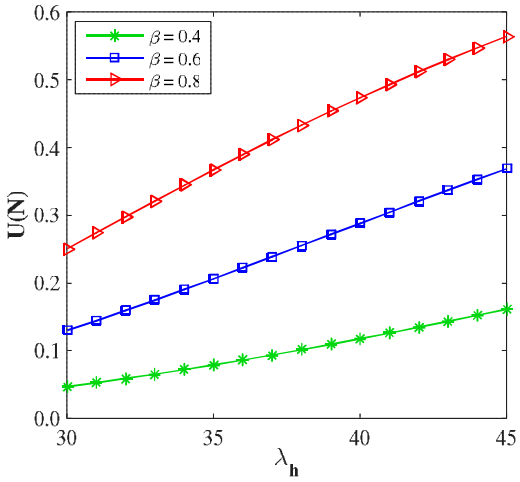

Figure 3.14: Buffer utilization as a function of handoff arrival rate for different queueing probabilities.

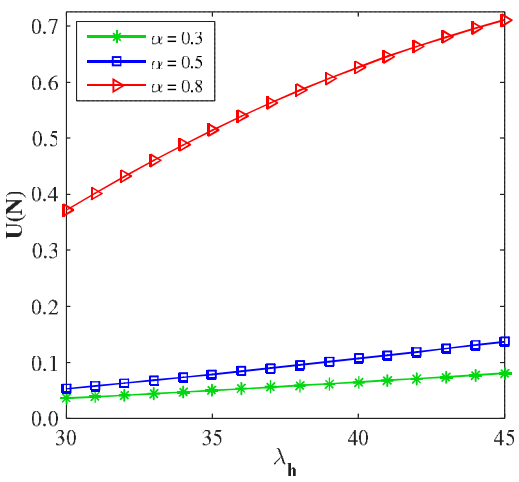

Figure 3.15: Buffer utilization as a function of handoff arrival rate for different signal quality probabilities.

probability, β allows more handoff calls to wait in the buffer, thereby, leads to higher buffer utilization factor, as illustrated in Fig. 3.14. Further, it can be observed in Fig. 3.15 that the buffer utilization is more sensitive to the signal quality for higher values of α. With an increase in the probability of an incoming handoff call to be of good quality, more handoff calls occupy the space in buffer and thus results in higher utilization factor. This is because the handoff calls are prioritized by allowing them to be queued in a finite buffer and good quality calls reside in the cell for a longer duration than the poor quality calls.

Next, we discuss how the size of the buffer, N and handoff arrival rate, λ_h behave under various scenarios. Since with an increase in the buffer size, larger delay of calls is expected, thus determining the buffer size based on channel occupancy levels can result in very long waiting times for calls, as discussed by Samba et al. [203]. Thereby, the QoS perceived by the users is evaluated in terms of throughput and delay of handoff calls. Evaluation of these QoS indices is particularly important for evaluating the maximal buffer size and appropriate handoff arrival rate for which the throughput attains maximum value.

We notice from Fig. 3.16 that the average packet delay shows little sign of saturation

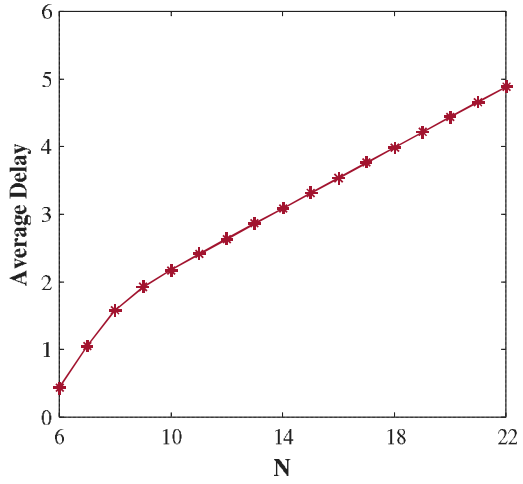

Figure 3.16: Average delay as a function of number of channels.

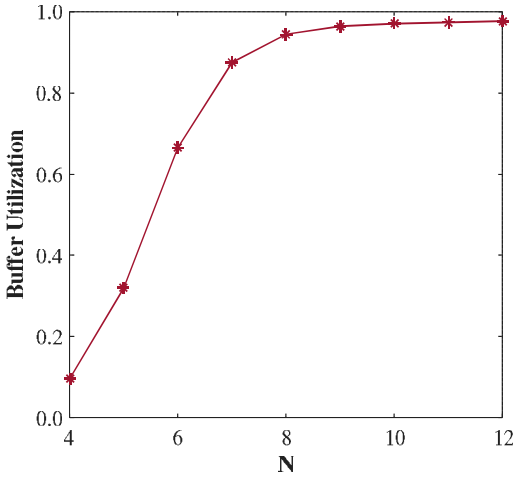

Figure 3.17: Buffer utilization as a function of number of channels.

and increases with the increase in buffer size. However, considering the measure buffer utilization gives an idea for the maximum bound of buffer size as shown in Fig. 3.17. Likewise, Fig. 3.18 below demonstrates that the average delay of handoff calls increases with increased input traffic since the buffer starts to fill up. Moreover, having found the throughput of handoff calls as depicted in Fig. 3.19, we can determine the appropriate handoff arrival rate for which the throughput attains the maximum value.

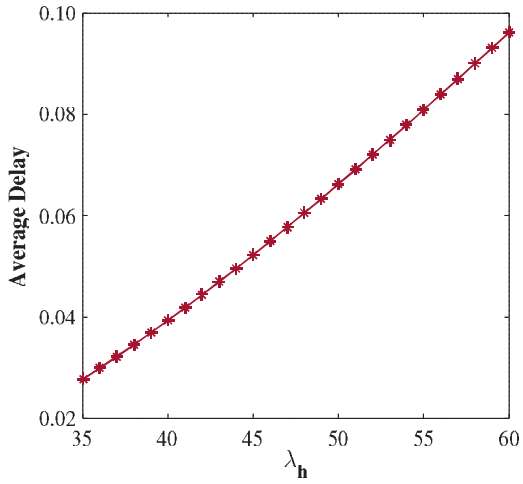

Figure 3.18: Average delay as a function of handoff arrival rate.

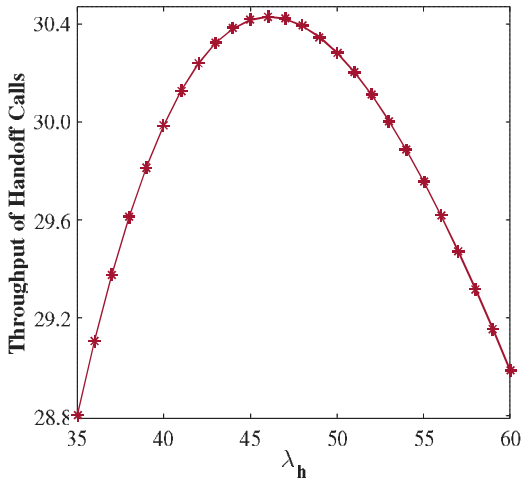

Figure 3.19: Throughput of handoff calls as a function of handoff arrival rate.

Further, following the algorithm given in Section 3.5, Fig. 3.20 is depicting the opti-

mized values of γ^* in presence of a hard constraint $B_h \leq P_h$ by varying $0.008 \leq P_h \leq 0.04$. For the presented results, we assume that each cell has 15 full duplex channels ($S = 15$), new call arrival rate, λ_n is fixed to 35, handoff call arrival rate, λ_h is fixed to 30, $\mu = 2$, $\mu_3 = 2$, $\alpha = 0.5$ and $\beta = 0.2$. The number of guard channels, C for FGC policy is set to 4 and the buffer size, N for handoff requests is set to 3. At each obtained value of γ^*, the equivalent value of blocking probability, B_n and dropping probability, B_h are determined. In consequence, the illustrated results in Fig. 3.20 may be used to provide the minimum blocking probability corresponding to a specified level of QoS for the dropping probability of handoff calls. As an example, for required P_h to be 3% as a QoS measure, the optimized γ^* is 0.75 which provides the blocking probability as 27%.

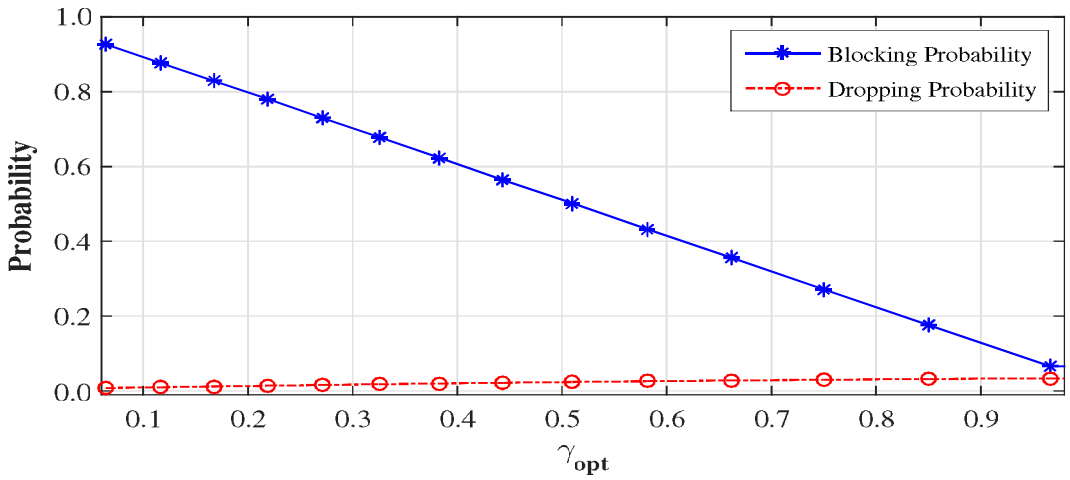

Figure 3.20: Blocking and dropping probability as a function of optimized value γ^*.

3.7 Chapter Summary

In this chapter, we have investigated the effect of signal quality under the joint utilization of the FGC scheme and the queueing scheme. CTMC models are developed to analyze the proposed CAC schemes. The suggested re-handoff decision of poor quality calls gives an additional benefit to establish a communication link with the neighboring BS to get better service. The derived product type formulae for steady-state probabilities easily allows us to compute the performance measures of the system. It is revealed from the

analysis carried out in this work that the good trade-off between the blocking probability of new calls and the dropping probability of handoff calls is achieved while maximizing resource utilization. In case of heavy handoff traffic, the proposed model II provides better performance in QoS and efficient utilization of limited channel resources compared to the proposed model I. Results have also shown that the integration of buffer in the proposed schemes outperforms the existing ones without any buffer. The appropriate values of maximal bound for buffer size and handoff arrival rate in order to minimize the queue delay and to maximize the queue throughput are obtained, respectively. Furthermore, the optimal value of acceptance probability for a new call is obtained to minimize the new call blocking probability under a hard constraint on handoff dropping probability.

Chapter 4

Joint Analysis of Spectrum Sensing and Access in CRNs

"Even imperfection itself may have its ideal or perfect state."
— Thomas De Quincey

4.1 Introduction

As discussed in Chapter 1, spectrum sensing is the crucial functionality in the operation of cognitive radio networks (CRNs), enabling to use the best spectrum opportunities with minimal interference on licensed user signals. However, opportunistic access with interference avoidance faces a multitude of challenges in determining the spectrum holes and detecting the presence of primary user (PU) in a multiuser environment. Perfect sensing is a useful assumption for tractable analysis of dynamic spectrum access (DSA) systems. Though it is easier to construct a model with perfect sensing but being an impractical scenario, it casts doubts on the accuracy of such a model. The imperfect spectrum sensing significantly affects the system performance, hence its impact cannot be ignored. Much research on sensing or detection methods has been done in the literature (e.g., see Kay [204]; Kim and Shin [205]; Maleki et al. [206]) however, it is not the focus in this

work. No matter what spectrum sensing method is used, the spectrum sensing outcomes cannot be perfect and leads to some sensing errors. We conduct our research to see the effectiveness of prominent sensing errors i.e. false alarms and mis-detections. The false alarm of PUs' presence on the channel restricts the secondary users (SUs) to access the channel which results in resource wastage i.e. spectrum wastage. On the other hand, the mis-detection enables SUs to establish communication simultaneous to the PUs which results in data-collision/loss along with the interference at PU.

A serial transmitting-sensing based approach has been studied by Yucek and Arslan [207], where sensing is performed by the incoming SUs before transmission. However, according to Heo et al. [208], to enhance the SUs' throughput and appropriately protect the PUs, SUs should perform spectrum sensing on a continuous basis during their ongoing transmission as well. As we discussed earlier, an important issue while performing continuous sensing is the false alarm rate (FAR), which is addressed in the present work. The frequent occurrence of false alarms makes it challenging for SUs to efficiently explore and utilize the spectrum opportunities and thereby degrades their quality of service (QoS). In order to characterize false alarm occurrences for ongoing SUs, we consider the average number of false alarms per unit time, modeled by a Poisson process (see e.g., Lee and Jang [209]; Suliman et al. [210]).

Different DSA strategies have been proposed in the literature, including by Zhang et al. [211] and Song et al. [212]. Recently, Lee and Yeo [213] presented the analysis of channel availability by employing spectrum handoff under unreliable sensing. The results depict that execution of scheme with spectrum handoff results in higher channel availability than not executing spectrum handoff. However, the blocking probability and the forced dropping probability of SUs grow rapidly with the increment in arrival rates of PU and SU. Thus, how to diminish probabilities of blocking and forced dropping for SUs despite higher user arrival rates brings up an interesting question.

Motivated by these observations, we propose in this chapter a new queue-based spectrum access strategy supporting heterogeneous users under imperfect spectrum sensing. The proposed scheme aims to enhance the performance of CRNs by providing SUs with

the ability of dynamically seeking and exploiting opportunities without interfering with PUs. In brief, the main contributions of the work in this chapter are summarized as follows:

1. A joint analysis of spectrum sensing and spectrum access mechanisms is performed. To investigate the effect of imperfect spectrum sensing, an analytical frame structure is developed for heterogeneous traffic in CRNs wherein the data transmission and sensing are the parallel phenomenon. Unlike existing works, the proposed strategy thoroughly investigates the effect of sensing errors including FARs on the performance of CRNs by taking state-dependent (i.e., depending on the current state) transition rates into account.

2. A queue-based solution is developed to reduce the blocking probability and the forced dropping probability considering two types of SUs i.e. real-time SUs (RSUs) and non real-time SUs (NRSUs). We introduce two buffers that are dedicated for allocation to newly arriving NRSUs and interrupted NRSUs performing handoff, respectively.

3. To further enhance the throughput of SUs, p-retry policy is utilized for queueing in the proposed scheme.

The remainder of this chapter is organized as follows. An overview of the related work is given in Section 4.2. In Section 4.3, the system model is presented, together with assumptions. Section 4.4 describes the proposed scheme and an extensive analytical model based on five-dimensional continuous-time Markov chain (CTMC). The performance metrics are derived in Section 4.5. In Section 4.6, we present and discuss the main numerical results and thereafter conclude the chapter in Section 4.7.

4.2 Related Work

To detect the appearance of PU in CRNs, several studies have been proposed in recent years. For instance, in order to minimize the interference on returning PUs, Kim and

Shin [214] investigated the issues of maximizing the overall discovery of opportunities in the available spectrum and minimizing the delay in locating a vacant channel. Liang et al. [215] formulated a sensing throughput trade-off problem to maximize the achievable throughput for the SUs under the constraint that the PUs are sufficiently protected. A queueing framework was developed for joint spectrum sensing and access by El-Sherif and Liu [216], considering the effect of spectrum sensing errors on the performance of the SUs' multiple channel access. Although the problem of interference is addressed in these works, contrary to our study, the underlying assumption made therein is that spectrum sensing and data transmission cannot be carried out simultaneously. That is, in order to perform sensing, it requires SU to periodically suspend its data transmission which results in the reduction of SUs' throughput. Additionally, the detection accuracy is also questionable in this technique as the sensing time duration is rather limited.

To address this issue, the approach of simultaneous sensing and data transmission has been studied by a few authors. For instance, Thakur et al. [217] analyzed the effect of imperfect sensing monitoring in high-traffic CRNs. Despite considering the challenge of unnecessary false alarms, Liao et al. [218] and Chang et al. [219] did not analyze its impact on performance metrics such as throughput, blocking, termination and dropping probabilities. Further, several types of unreliable sensing for both incoming and ongoing SUs were analyzed by Tang and Xie [220] and Tang et al. [221]. Therein, a buffer is employed for ongoing SUs and the effect of different sensing techniques on the performance of CRNs is investigated. However, in all the aforementioned work the problem of the FAR has not been investigated and the work is limited to homogeneous traffic of SUs.

To reflect the realistic situation of delayed network access and to reduce the blocking and forced termination probabilities, designing effective queueing disciplines in CRNs also has gained importance (see e.g., Palunčić [222]). Due to the preempted priority of PUs, the transmission of a SU is possible to get interrupted by a newly arriving PU. Once interrupted, the SU can either leave the system or wait in a buffer so that its connection is terminated or suspended. Some existing works e.g., of Chu et al. [223] and Suliman et al. [210], assumed the forced termination of interrupted SUs' connection which results